

## Emission spectra of an atom in a cavity in the presence of a squeezed vacuum

J. Gea-Banacloche,\* R. R. Schlicher, and M. S. Zubairy†

*Max-Planck-Institut für Quantenoptik, D-8046 Garching, Federal Republic of Germany*

(Received 29 January 1988)

We have investigated the interaction of a single atom with a single mode of the radiation field in an ideal cavity when the field is initially in a squeezed-vacuum state. In particular, we present results for the spectrum of the emitted light and for the time evolution of the squeezing inside the cavity. Our results contrast sharply with previous studies of single two-level atom interaction with a continuum of squeezed-vacuum modes. In particular, the results are shown to be insensitive to the initial phase of the atomic dipole relative to the squeezed field, and the squeezing is destroyed by the coherent interaction, in a time essentially independent of the initial degree of squeezing. Most features of the spectrum are very similar to those predicted for an initial thermal state, although the two-peaked structure associated with vacuum-field Rabi splitting is more apparent for a squeezed state with a small average number of photons than for a thermal state with the same number of photons.

### I. INTRODUCTION

The interaction of an atom with an optical field in a squeezed state was the subject of a large amount of theoretical work in the past two years, coinciding with the first experimental observations of squeezed light.<sup>1</sup> Gardiner<sup>2</sup> calculated the spontaneous decay of an atom in a squeezed-field environment, and Carmichael, Lane, and Walls<sup>3</sup> have recently obtained the fluorescence spectrum of such an atom. Ritsch and Zoller<sup>4</sup> have in turn calculated the absorption spectrum of this system.

In all these studies the ordinary vacuum seen by the atom is replaced by a multimode "squeezed vacuum." That is, every single mode of the field with which the atom might interact (except for the driving and probe fields in the fluorescence and absorption problems) is assumed to be squeezed. Alternatively, as pointed out by Gardiner,<sup>2</sup> in the dipole approximation it is enough to assume that the atom is interacting with a pure, squeezed, dipole wave. Some very interesting deviations from the ordinary decay and ordinary emission and absorption spectra in a normal vacuum environment are obtained under such conditions. In particular, the decay rate of the atomic dipole is seen to depend on its phase relative to the squeezed field, and the width of the absorption and emission spectra also depends on the relative phase between the driving coherent field and the squeezed field. Subnatural linewidths are possible for some cases.

However, the experimental realization of such a squeezed-vacuum environment for an atom in free space may prove difficult. It seems natural to investigate, as an alternative problem, what happens when the atom interacts with a single-mode squeezed field in a cavity. Changes in the characteristics of the spontaneous radiation have recently been predicted for a collection of atoms in a laser cavity into which squeezed light is injected to couple to the lasing mode.<sup>5</sup> These atoms, of course, still interact with a continuum of vacuum modes (in

directions other than that of the lasing mode). Instead, what we propose to investigate here is the behavior of a single atom in an ideal cavity which supports only a single mode, i.e., the Jaynes-Cummings model<sup>6</sup> with a squeezed field.

The main difference between this system and the ones investigated in Refs. 2–4 is that it is a closed system, where, if the cavity losses are negligible, the light radiated by the atom is eventually reabsorbed and reemitted. As a result, the reaction of the atom back on the initially squeezed field cannot be neglected. As we shall show below, this leads to results substantially different from the open (irreversible) systems.<sup>2–4</sup> We should mention that some work on this system already exists,<sup>7</sup> although only the time evolution of the atomic inversion has been previously reported. There is also related work on the generation of a squeezed field in a cavity by an atom initially excited, or in a coherent superposition of states.<sup>8–11</sup> Here we concentrate on the emission spectrum of the atom in the cavity, along the lines of the work by Narozhny, Sánchez-Mondragón, and Eberly,<sup>12,13</sup> who studied the case when the cavity initially contains a coherent state.

The main difficulty with the assumption of a perfect cavity is, of course, obvious: namely, that it is impossible to observe the spectrum of the emitted light directly without introducing some losses. We do not think, however, that this is a major problem, because some recent work involving atoms in nonideal cavities<sup>14</sup> shows that for small enough losses the spectrum of the transmitted light is indeed very close to the one calculated for the ideal cavity.

Our paper is organized as follows. In Sec. II we generalize some of the results of Ref. 13 to the case when the single-mode field inside the cavity is in an arbitrary quantum state. Then we specialize to the case of a "squeezed-vacuum" state, which yields a somewhat unexpected result, namely, an insensitivity to the relative phase between the atomic dipole and the squeezed field, in marked contrast to the results of Refs. 2 and 3. In Sec. III we

show some of the calculated spectra and compare them to those obtained for fields initially in a thermal or a coherent state. The comparison is relevant because a squeezed-vacuum field does have a nonzero average number of photons. We discuss the results in terms of the spectra appropriate to initial pure-number states, presented in Sec. II. In Sec. IV we illustrate the reaction of the atom back on the field by showing how the degree of squeezing of the field in the cavity evolves with time. Finally, Sec. V contains a discussion and conclusions.

## II. SPECTRUM FOR AN ARBITRARY INITIAL STATE

The system we consider here is essentially the Jaynes-Cummings model:<sup>6</sup> a single two-level atom interacting, in the rotating-wave approximation, with a single mode of the electromagnetic field. The well-known Hamiltonian for this model is

$$H = \frac{1}{2}\hbar\omega_a\sigma_3 + \hbar\omega_c(a^\dagger a + \frac{1}{2}) + \hbar\lambda(a^\dagger\sigma + \sigma^\dagger a), \quad (1)$$

where  $\omega_a$  is the frequency of the atomic transition,  $\omega_c$  the

$$S(\omega) = 2\Gamma \int_0^T dt_1 \int_0^T dt_2 e^{-(\Gamma-i\omega)(T-t_1) - (\Gamma+i\omega)(T-t_2)} \langle \xi, \psi | \sigma^\dagger(t_1)\sigma(t_2) | \xi, \psi \rangle, \quad (3)$$

which can easily be shown to be equivalent to the time-ordered expression used in Ref. 13. Here  $T$  is the time at which the measurement takes place and  $1/\Gamma$  is the filter's response time.

We have used the expression for  $\sigma(t)$  given in Ref. 12 to evaluate Eq. (3) for an arbitrary initial state  $|\xi\rangle$  of the field (only the result for an initial coherent state was given in Ref. 13). The details of the calculation may be found in the Appendix. We find that the spectrum may be expressed in terms of the photon number distribution  $P_n$  of the initial field state and of certain functions  $\mathcal{F}_n(\omega)$  which are simply the spectrum for an initial pure number state  $|n\rangle$ . For an atom initially in an excited state, the result is

$$S^{(+)}(\omega) = \sum_{n=0}^{\infty} P_n \mathcal{F}_n^{(+)}(\omega). \quad (4a)$$

For an atom initially in the ground state, the result is instead

$$S^{(-)}(\omega) = \sum_{n=0}^{\infty} P_{n+1} \mathcal{F}_n^{(-)}(\omega) \quad (4b)$$

with

$$\begin{aligned} \mathcal{F}_n^{(\pm)}(\omega) = \frac{\Gamma}{4} [ & |F_n^{(\pm)}(\mu_n, \mu'_n) + F_n^{(\pm)}(-\mu_n, \mu'_n)|^2 \\ & + |F_n^{(\pm)}(\mu_n, -\mu'_n) \\ & + F_n^{(\pm)}(-\mu_n, -\mu'_n)|^2 ]. \end{aligned} \quad (5)$$

frequency of the cavity eigenmode,

$$\sigma_3 = |a\rangle\langle a| - |b\rangle\langle b|$$

( $|a\rangle$  and  $|b\rangle$  are the upper and lower atomic states, respectively),  $\sigma = |b\rangle\langle a|$ , and  $\lambda$  is the atom-field coupling constant.

Exact solutions for the time evolution of the various operators appearing in Eq. (1) (in the Heisenberg picture) are available.<sup>12,15</sup> We shall use them to compute the spectrum of the radiation emitted by the atom, which we take to be given by the convolution of the dipole-dipole correlation function

$$\langle \xi, \psi | \sigma^\dagger(t)\sigma(t') | \xi, \psi \rangle \quad (2)$$

with the Fourier transform of the filter's spectral transmission function taken at the times  $t$  and  $t'$ . In Eq. (2)  $|\xi\rangle$  is the initial state of the radiation field, and  $|\psi\rangle$  the initial state of the atom (which could be  $|a\rangle$ ,  $|b\rangle$ , or a linear superposition of them).

The physical transient spectrum<sup>16</sup> is then given by the expression

The functions  $F_n^{(\pm)}$  are given by

$$\begin{aligned} F_n^{(+)}(\mu_n, \mu'_n) = & \left[ 1 + \frac{\Delta}{2\mu_n} \right] \left[ 1 + \frac{\Delta}{2\mu'_n} \right]^{1/2} \\ & \times \frac{e^{i(\mu_n + \mu'_n - \omega + \omega_c)T} - e^{-\Gamma T}}{\Gamma + i(\mu_n + \mu'_n - \omega + \omega_c)}, \end{aligned} \quad (6a)$$

$$\begin{aligned} F_n^{(-)}(\mu_n, \mu'_n) = & \frac{\lambda\sqrt{n+1}}{\mu_n} \left[ 1 + \frac{\Delta}{2\mu'_n} \right]^{1/2} \\ & \times \frac{e^{i(\mu_n + \mu'_n - \omega + \omega_c)T} - e^{-\Gamma T}}{\Gamma + i(\mu_n + \mu'_n - \omega + \omega_c)}. \end{aligned} \quad (6b)$$

with the arguments

$$\mu_n = [(\Delta/2)^2 + (n+1)\lambda^2]^{1/2}, \quad (7a)$$

$$\mu'_n = [(\Delta/2)^2 + n\lambda^2]^{1/2}. \quad (7b)$$

Here  $\Delta = \omega_a - \omega_c$  is the detuning between the atomic and the cavity frequencies. The arguments  $\mu_n$  and  $\mu'_n$  are generalized Rabi frequencies for number states  $|n+1\rangle$  and  $|n\rangle$ .

As shown in the Appendix, if the atom is initially in a coherent superposition of the states  $|a\rangle$  and  $|b\rangle$ ,  $|\psi\rangle = \alpha|a\rangle + \beta|b\rangle$ , the spectrum is given by the general result

$$\begin{aligned} S(\omega) = \frac{\Gamma}{4} \sum_{n=0}^{\infty} & |\alpha^* \langle \xi | n \rangle [F_n^{(+)}(\mu_n, \mu'_n) + F_n^{(+)}(-\mu_n, \mu'_n)] + \beta^* \langle \xi | n+1 \rangle [F_n^{(-)}(\mu_n, \mu'_n) + F_n^{(-)}(-\mu_n, \mu'_n)]|^2 \\ & + (\mu'_n \rightarrow -\mu'_n), \end{aligned} \quad (8)$$

which is seen to reduce to Eqs. (4) in the special cases when either  $\alpha$  or  $\beta$  are zero, since the photon number distribution  $P_n$  is defined as

$$P_n = |\langle n | \xi \rangle|^2. \quad (9)$$

Equation (8) shows that in general the spectrum will depend on the relative phase of the atomic wave functions  $|a\rangle$  and  $|b\rangle$ , because of the presence of interference terms proportional to  $\alpha\beta^*$  and  $\alpha^*\beta$ . The phase of  $\alpha\beta^*$  is the phase of the atomic dipole, and the interference terms contain the difference between this phase and that of the cavity field.

In the case of the initial cavity field being in a squeezed-vacuum state, however, no such phase dependence is obtained. This result follows immediately from the expression of a squeezed-vacuum state in the basis of photon number eigenstates:

$$|\xi\rangle_{\text{sq. vac.}} = \sum_{n=0}^{\infty} \frac{(-1)^n e^{-in\phi}}{\sqrt{\cosh r}} \frac{\sqrt{(2n)!}}{2^n n!} (\tanh r)^n |2n\rangle, \quad (10)$$

where  $r$  is the squeezing parameter ( $r=0$  for ordinary vacuum).

Equation (10) shows that the only number states which are found in a squeezed-vacuum state are those which have an even number of photons (the alternative designation "two-photon coherent states" immediately comes to mind at this point). This means that there is no value of  $n$  for which both  $\langle n | \xi \rangle$  and  $\langle n+1 | \xi \rangle$  in Eq. (8) are nonzero, and thus there are no interference terms. The spectrum (8) contains only terms proportional to  $|\alpha|^2$  and  $|\beta|^2$ , the relative weights of  $|a\rangle$  and  $|b\rangle$  in the initial state. A statistical mixture of  $|a\rangle$  and  $|b\rangle$  with totally random phases would therefore yield the same spectrum as a phased coherent superposition.

This result is all the more surprising in view of the results reported in Refs. 2-4, where phase sensitivity plays a major role. For instance, in Ref. 2 it was found that for an atom excited into a coherent superposition and interacting with a squeezed vacuum the decay rates of the states  $1/\sqrt{2}(|a\rangle + e^{i\phi}|b\rangle)$  and  $1/\sqrt{2}(|a\rangle - e^{i\phi}|b\rangle)$  are different. Similarly Refs. 3 and 4 report different linewidths for different relative phases between the field which drives the atomic dipole and the squeeze field.

In contrast, the phase sensitivity is totally absent in the problem at hand. This is obviously related to the two-photon character of the squeezed state. The atomic transition is a single-photon transition, and our results suggest that it cannot interact coherently with a *single-mode* squeezed vacuum. All that matters is the number of photons in the field, which are absorbed or emitted one at a time. Indeed, when the interference terms in Eq. (8) vanish, the result depends only on the photon number distribution  $P_n$ , that is, on the magnitudes of the coefficients  $\langle n | \xi \rangle$ , and not on their phases.

It should be mentioned at this point as well, that the insensitivity to the initial relative phase in this problem extends also to the correlation functions of the form  $\langle \sigma\sigma \rangle$  and  $\langle aa \rangle$  associated with the quadrature components of the field: They also turn out to depend only

on  $|\alpha|^2$  and  $|\beta|^2$  when the initial state of the field is the squeezed vacuum (10).

For the remainder of this paper we shall concentrate on the emission spectrum, with the atom initially excited. The results for an atom initially in the ground state turn out not to be very different qualitatively (except, of course, when the initial field in the cavity is taken to be the vacuum state, in which case nothing happens, since the atom cannot absorb energy from the vacuum).

The spectrum (4a) is seen to be a weighted average of the spectra  $\mathcal{F}_n^{(+)}$  for pure-number states, with the weight function being the photon number distribution. Many of its features may, therefore, be understood from a consideration of the spectra  $\mathcal{F}_n^{(+)}$ . These are plotted in Fig. 1.

The spectrum for the initial state  $|0\rangle$  in Fig. 1 shows the so-called vacuum-field Rabi splitting. The function  $F_n^{(+)}$  in Eq. (6a) has a peak when  $\omega - \omega_c = \mu_n + \mu'_n$ . In the spectral function  $\mathcal{F}_n^{(+)}$  [Eq. (5)] the arguments  $\mu_n$  and  $\mu'_n$  appear with all the possible sign combinations, which suggests that in general the spectrum for an initial state  $|n\rangle$  will consist of four peaks. For the state  $|0\rangle$ , however, and in the absence of detuning ( $\Delta=0$ ), we have  $\mu'_n=0$ , so that  $\mu_n - \mu'_n = \mu_n + \mu'_n$  and  $-\mu_n - \mu'_n = -\mu_n + \mu'_n$ , giving only two peaks at  $\omega - \omega_c = \pm\lambda$ .

For any other initial number state  $|n\rangle$ ,  $n \neq 0$ , the spectrum shows either three or four peaks. For  $n \geq 1$ , the two peaks obtained for  $n=0$  split into two separate peaks each, one pair at  $\omega - \omega_c = \pm(\mu_n + \mu'_n)$  moving away from the cavity frequency  $\omega_c$  as  $n$  increases, while the other pair at  $\omega - \omega_c = \pm(\mu_n - \mu'_n)$  move closer together (towards  $\omega - \omega_c = 0$ ) as  $n$  increases. The three-peak spectrum arises for large photon numbers when the latter two peaks are eventually combined into what appears as a single peak for a finite-resolution spectrometer [the width of the peaks in Eq. (6) is equal to  $\Gamma$ , the spectrometer's resolution]. The other two peaks are centered at what is essentially the Rabi frequency  $2\lambda\sqrt{n}$  for a field of ampli-

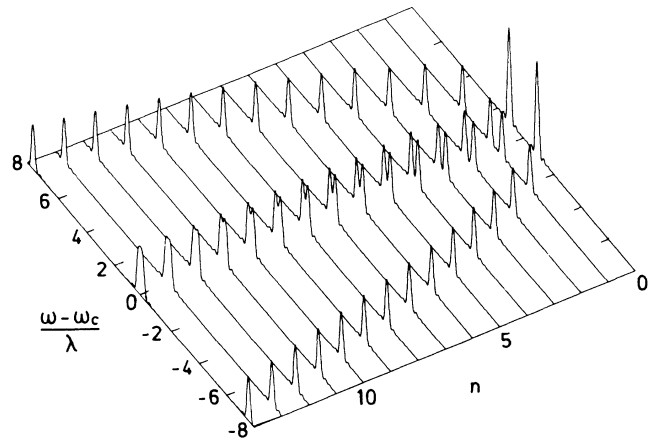


FIG. 1. The functions  $\mathcal{F}_n^{(+)}(\omega)$  which appear in Eq. (4a), and which correspond to the spectrum of the light emitted when the initial state of the field is a pure number state  $|n\rangle$ . The interaction time  $T=20\lambda^{-1}$ , and the assumed resolution of the spectrometer  $\Gamma=0.02\lambda$ , so that  $\Gamma T=0.4$ . No detuning ( $\Delta=0$ ).

tude  $\sqrt{n}$ . In this way, for large photon numbers, one obtains the basic shape of the (semiclassical) three-peaked spectrum of resonance fluorescence.

We are especially interested in any nonclassical effects that the system with an initially squeezed state might exhibit. We turn to this in the next section.

### III. EMISSION SPECTRA

Figure 2 shows the emission spectra, calculated from the equations presented in the previous section, for a single atom in a cavity which initially contains a squeezed vacuum state, a thermal state, and a coherent state, respectively. We have calculated the spectra, in each case, for different values of the average photon number in the initial state. This is because, from the discussion in Sec. II, we expect the photon number distribution to play a

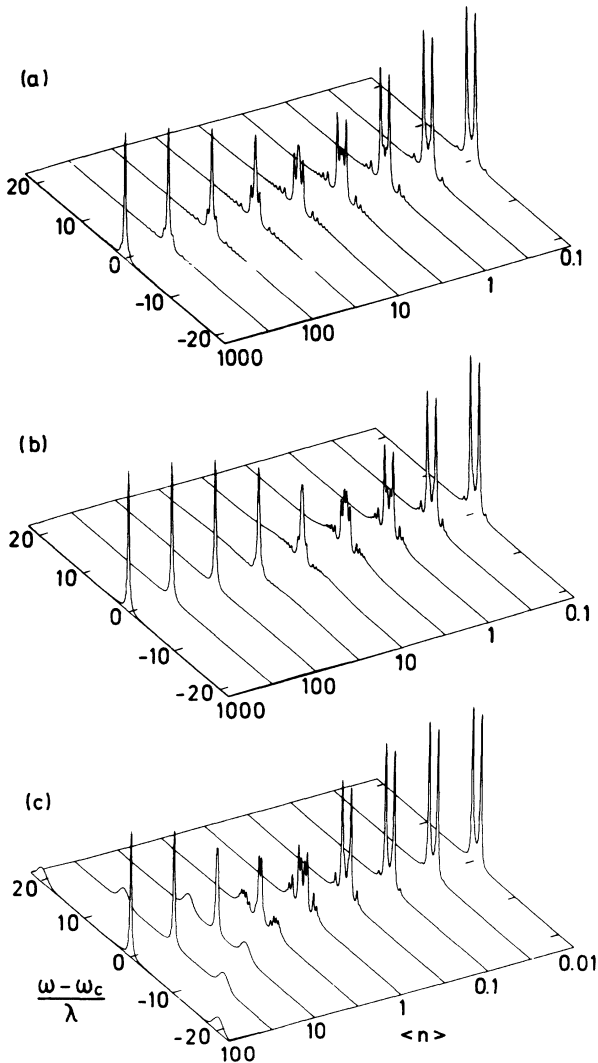


FIG. 2. Emission spectrum for the cavity field initially in a squeezed-vacuum state (a), thermal field (b), and coherent state (c), plotted in each case as a function of the frequency and the average number of photons  $\langle n \rangle$  in the field. Squeezed-vacuum state:  $\langle n \rangle = \sinh^2 r$ ; thermal field:  $\langle n \rangle = [\exp(\hbar\omega/kT) - 1]^{-1}$ ; coherent state:  $\langle n \rangle = |\alpha|^2$ . Interaction time  $T = 20\lambda$ , resolution of spectrometer  $\Gamma = 0.2\lambda^{-1}$ , so that  $\Gamma T = 4$ . No detuning ( $\Delta = 0$ ). Note the scale for  $\langle n \rangle$  is different in (c).

decisive role, so the spectra for the different states should be compared for the same average number of photons.

For the squeezed vacuum, the photon number distribution is easily obtained from Eq. (10). The average number of photons increases with the squeezing parameter  $r$ : it is given by  $\langle n \rangle = \sinh^2 r$ . In terms of this average value, the photon number distribution may be written as

$$P_{2n} = \frac{1}{\sqrt{\langle n \rangle + 1}} \frac{(2n)!}{2^{2n}(n!)^2} \left[ \frac{\langle n \rangle}{\langle n \rangle + 1} \right]^n, \quad (11)$$

$$P_{2n+1} = 0.$$

In this form, the photon distribution resembles very much that of a thermal state,

$$P_n^{\text{thermal}} = \frac{1}{\langle n \rangle + 1} \left[ \frac{\langle n \rangle}{\langle n \rangle + 1} \right]^n, \quad (12)$$

except for the absence of all the odd terms, and the prefactor  $(2n)!/2^{2n}(n!)^2$  in (11). This factor decays for increasing  $n$ , although very slowly (from Stirling's formula it may be seen to go as  $n^{-1/2}$ ). For  $n=0,1,2,3,4,\dots$ , its value is 1, 0.5, 0.38, 0.31, 0.27,  $\dots$ , respectively. This gives the distribution (11) a rather sharp peak at  $n=0$  (regardless of the value of  $\langle n \rangle$ ,  $P_4$  is already down by a factor of  $1/e$  from  $P_0$ ), but a long tail, very similar to that of a thermal state.

This simple observation, together with the spectra for the pure number states  $|n\rangle$  plotted in Fig. 1, allows one to readily understand the main features of Fig. 2. In particular, one can see that the vacuum-field Rabi splitting peaks in the spectrum for the squeezed-vacuum field persist for larger values of the average photon number than they do for the corresponding thermal state. This is due to the larger relative weight of the vacuum state in the distribution (11) than in the distribution (12).

As the average number of photons increases, the distributions (11) and (12) become broader [ $\Delta n^2$  increases as  $2\langle n \rangle(\langle n \rangle + 1)$  for (11) and as  $\langle n \rangle(\langle n \rangle + 1)$  for (12)], so more of the functions  $\mathcal{F}_n$  shown in Fig. 1 become important in the calculation of the spectrum (4a). Thus eventually the double peak of the vacuum Rabi splitting is washed out. Yet, because the photon distributions (11) and (12) are very broad (and have no peaks, other than the one at  $n=0$ ), no coherent sidebands emerge for either the squeezed or the thermal states.

The picture is different for a coherent state. Here the photon number distribution does have a maximum, around  $n = \langle n \rangle$ , and a much smaller average width  $\Delta n$ , of the order of  $\sqrt{\langle n \rangle}$  (as opposed to  $\sim \langle n \rangle$  for the squeezed-vacuum and thermal states). The relative weight of the vacuum state diminishes rapidly as the average number of photons increases: Thus the double peak in the spectrum associated with the vacuum disappears much more rapidly (note the different scale used for the coherent state in Fig. 2). Coherent sidebands do appear, centered, as Fig. 2 shows, near  $\omega - \omega_c = 2\lambda\sqrt{\langle n \rangle}$ . The width of the sidebands reflects the width of the photon number distribution: About  $\sqrt{\langle n \rangle}$  states, around the state having  $n = \langle n \rangle$ , contribute to the final spectrum, and their sidebands are all at slightly different values, as

Fig. 1 shows. [We have

$$(\langle n \rangle \pm \sqrt{\langle n \rangle})^{1/2} \simeq \sqrt{\langle n \rangle} \pm \frac{1}{2},$$

so the width of the sidebands in Fig. 2(c) should be of the order of  $2\lambda$ , independent of  $\langle n \rangle$ .]

The width of the central peak, on the other hand, is, as before, determined only by the resolution of the detector. This means, of course, that even when the spectra in Fig. 2 look "classical" they really are not. The usual Mollow spectrum for an atom in free space<sup>17</sup> has precise values for the ratio of the heights of the peaks, which are broadened by the level lifetime (i.e., spontaneous emission). The different ratios of heights and the subnatural linewidths, which are obtained in the cavity case, arise from the suppression of spontaneous emission in all of the other field modes.

Yet, perhaps the most striking of the nonclassical features is the vacuum-field Rabi splitting. Our conclusion is that, if the average number of photons in the cavity is nonzero, this effect will be easiest to observe if the initial field is in a squeezed-vacuum rather than a thermal state, and least visible for an initial coherent state (compare, for instance, in Fig. 2 the spectra corresponding to  $\langle n \rangle = 10$  for the three kinds of states), but that it is inevitably washed out for large average number of photons (also for pure number states, as Fig. 1 shows).

Figure 2 was computed for zero detuning between the cavity and the atomic frequencies. Figure 3 shows what happens when the field and the atom are not in resonance, for the case when the initial state is a squeezed vacuum. The detuning has been chosen to be  $\omega_a - \omega_c = 5\lambda$ . It is seen that when the number of photons in the field is small, the spectrum is mostly centered around  $\omega = \omega_c + 5\lambda = \omega_a$ , but that as  $\langle n \rangle$  increases the stimulated emission peak at  $\omega = \omega_c$  becomes dominant.

This transition from mostly spontaneous to mostly stimulated emission can also be seen when the calculation is done with a coherent or a thermal state. When compared with a thermal state, the squeezed-vacuum spectrum shows more structure around the fluorescence peak

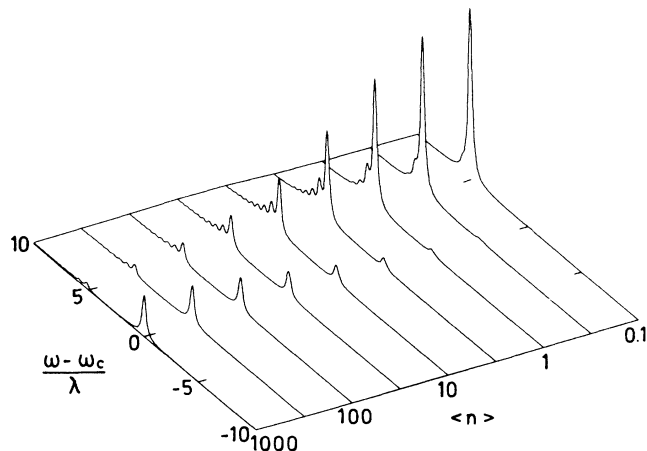


FIG. 3. The spectrum for an initial squeezed vacuum when the detuning  $\Delta = 5\lambda$  (other parameters as in Fig. 2).

(the oscillations in the high-frequency tail of this peak in Fig. 3 do not show for a thermal field); also, this peak survives for larger values of  $\langle n \rangle$  in the squeezed vacuum than in the thermal state. This is due again to the larger weight of the states with low photon numbers in the squeezed-state distribution (11). For a coherent state, on the other hand, the fluorescence peak obtained for small  $\langle n \rangle$  never quite disappears as  $\langle n \rangle$  is increased, but, rather it is shifted and eventually turns into a sideband at a distance

$$2[(\omega_a - \omega_c)^2/4 + \lambda^2 \langle n \rangle]^{1/2}$$

away from  $\omega_c$ .

#### IV. TIME EVOLUTION OF THE SQUEEZING IN THE CAVITY

The dipole-dipole correlation function (3) provides the spectrum of the light emitted by the atom. This is added to the field originally present in the cavity and modifies it. In this section we investigate how the properties of the total field in the cavity change as a result of the interaction with the atom. We find, in particular, that an initially squeezed field does not remain squeezed for very long.

The density operator of the field as a function of time is given by<sup>8</sup>

$$\begin{aligned} \rho_f(t) = & \cos[\lambda t (aa^\dagger)^{1/2}] \rho_f(0) \cos[\lambda t (aa^\dagger)^{1/2}] \\ & + a^\dagger \frac{\sin[\lambda t (aa^\dagger)^{1/2}]}{(aa^\dagger)^{1/2}} \rho_f(0) \\ & \times \frac{\sin[\lambda t (aa^\dagger)^{1/2}]}{(aa^\dagger)^{1/2}} a. \end{aligned} \quad (13)$$

For a squeezed-vacuum state the uncertainty in the quadratures  $a_1$  and  $a_2$  is given by the expressions

$$(\Delta a_1)^2 = \frac{1}{4} + \frac{1}{2}(\langle a^\dagger a \rangle + \frac{1}{2}\langle a^2 + a^{\dagger 2} \rangle), \quad (14a)$$

$$(\Delta a_2)^2 = \frac{1}{4} + \frac{1}{2}(\langle a^\dagger a \rangle - \frac{1}{2}\langle a^2 + a^{\dagger 2} \rangle). \quad (14b)$$

Using the form (13) for the density operator, and the initial condition  $\rho(0) = |\xi\rangle\langle\xi|$ , where the state  $|\xi\rangle$  is a general state of the field, we find

$$\langle a^\dagger a \rangle = \langle n \rangle + \sum_{n=0}^{\infty} P_n \sin^2(\lambda t \sqrt{n+1}), \quad (15a)$$

$$\begin{aligned} \langle a^2 \rangle = & \sum_{n=0}^{\infty} \langle n+2 | \xi \rangle \langle \xi | n \rangle \sqrt{n+2} \\ & \times [\sqrt{n+1} \cos(\lambda t \sqrt{n+3}) \cos(\lambda t \sqrt{n+1}) \\ & + \sqrt{n+3} \sin(\lambda t \sqrt{n+3}) \\ & \times \sin(\lambda t \sqrt{n+1})]. \end{aligned} \quad (15b)$$

For a squeezed vacuum, the coefficients  $\langle n | \xi \rangle$  are given by Eq. (10). In the curves plotted in Fig. 4, we have assumed that we start with a state squeezed along the  $a_1$  axis, which corresponds to taking  $\phi = 0$  in Eq. (10). Thus at  $t=0$  the quadrature  $a_1$  has a (squared) uncertainty below the vacuum value  $\frac{1}{4}$ , and  $a_2$  a correspondingly larger one. Note that for an initial real vacuum state,

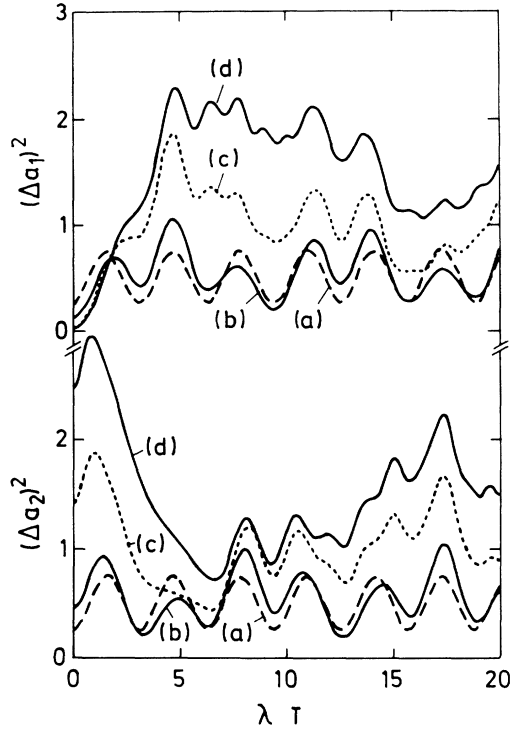


FIG. 4. Evolution of the squeezing in the cavity as a function of the interaction time. Atom initially in upper state, no detuning. The average number of photons in the field initially is (a) 0.0, (b) 0.1, (c) 1.0, (d) 2.0. The quadrature  $a_1$  is assumed to be squeezed initially. The field in the cavity is squeezed when either  $(\Delta a_1)^2$  or  $(\Delta a_2)^2$  drops below the value  $\frac{1}{4}$ , which corresponds to the minima of curve (a) in both figures (initial vacuum state).

(15b) is equal to zero and (15a) gives a purely sinusoidal time dependence with frequency  $\lambda$ , so that for that case ( $\langle n \rangle = 0$  in the figure) the noise in the quadratures, given by Eq. (14), oscillates between the values  $\frac{1}{4}$  and  $\frac{3}{4}$ .

The field in the cavity is only squeezed when the noise in one of the quadratures falls below the value  $\frac{1}{4}$ . The curve for an initial vacuum state, therefore, never exhibits squeezing, but it may be used as reference. We see that only for very low values of the average photon number in the initial state is the field squeezed at any times beyond the first few instants. Since larger values of the initial squeezing correspond to larger average photon numbers, we can see that the larger the initial squeezing is, the less squeezing is found at later times. In fact, for  $\langle n \rangle \geq 0.3$  the field never exhibits squeezing again, after the initial squeezing disappears. (In other words, we have not observed any “revivals of the squeezing” for  $\langle n \rangle \geq 0.3$ ).

This is in contrast with the results obtained in Ref. 8, where the initial state was taken to be a coherent state. There the field was seen to develop spontaneously some small amount of squeezing, which disappeared during the “collapse” times but returned during the “revivals.”

We see that the coupled evolution of the atom and the field substantially alters the properties of the latter, so that after a time of the order of  $1/\lambda$  the atom is not in-

teracting with a squeezed field anymore. This is very different from the situation envisioned in Refs. 2–4, where the reaction of the atom on the field is essentially negligible: The emitted photons escape the system and do not modify the multimode squeezed vacuum substantially. In our system, instead, the emitted photons are trapped within the cavity, and they destroy the squeezing very rapidly. A larger squeezing does not survive any longer, essentially because the larger average number of photons induces a larger emission rate.

## V. DISCUSSION

The main conclusion that can be drawn from the results presented here is that the evolution of the atom-field system composed of a two-level atom in an initially squeezed field is dramatically different when the system is placed in a single-mode cavity than it is when the system is open, and the squeezed field is broadband.<sup>2–4</sup>

The main differences are two. First, there is the total lack of sensitivity of this system to a possible phase difference between the atomic dipole and the squeezed field, due to the lack of coherent coupling between a single-photon transition and the two-photon state of the field that is a squeezed vacuum. Second, is the fact that the squeezing of the field is destroyed by the coupling very rapidly (in a time of the order of  $\lambda^{-1}$ ) regardless of the initial amount of squeezing present. This may be also due to the mismatched nature of the coupling.

The question immediately arises of how different the results would be with a two-photon transition: for instance, the generalized Jaynes-Cummings model where the transition is mediated by two photons of the cavity field and the atom consists of either two<sup>18,19</sup> or three<sup>20</sup> levels. These two-photon atomic systems indeed exhibit the phase sensitivity lacking in the present model. We will present the properties of the light generated in such a system in a future publication.

Concerning the spectrum of the emitted light, we have shown that it is determined solely by the photon statistics of the squeezed-vacuum state, and that it, therefore, has many features in common with what would be obtained for an initial thermal state (many more than for an initial coherent state) due to the broad nature of the photon distribution. The fact that the vacuum state has a larger relative weight in the makeup of a squeezed vacuum, however, allows for certain features, such as vacuum Rabi splitting, to be more prominent in the squeezed-vacuum state than in a thermal state with a comparable photon number.

We note that the similarity between the effects of a squeezed state and of a thermal state has already been realized in other physical systems.<sup>21</sup> (The results of Ref. 21 do suggest that the differences between a squeezed vacuum and a thermal field should be much more pronounced for the generalized multiphotons Jaynes-Cummings model than for the one-photon transition model considered here.) In the present system, the similarity between squeezed and thermal field was already pointed out by Milburn<sup>7</sup> in his discussion of the popula-

tion inversion (revivals). We have shown that this is due to the similarity between the respective photon distributions, and we expect that because of the nature of the coupling, a large number of effects in the interaction of two-level atoms with single-mode squeezed vacuum will, indeed, depend on the photon distribution only, with no coherent (off-diagonal) contributions.

Note that this is not necessarily the case in another type of system, the intermediate (and most common) case of an atom which interacts with a single-mode squeezed field, in a cavity perhaps, but which has also other decay channels available (to nonsqueezed vacuum modes). All the systems which are now used to generate squeezed light are of this third type, as are those studied, for instance, in Refs. 5, 9, and 11. In these systems the atom and the field may strongly influence each other, while retaining squeezing and phase sensitivity.

#### APPENDIX

The spectrum (3) may be calculated from the exact solutions for the Jaynes-Cummings model due to Ackerschalt<sup>15</sup> and presented in Ref. 12. Using the notation of that paper, with minor modifications, the operator  $\sigma(t)$  is given by

$$\sigma(t) = e^{-i\omega_c t} e^{iCt} \left[ \left[ \cos\gamma t + iC \frac{\sin\gamma t}{\gamma} \right] \sigma(0) - i\lambda \frac{\sin\gamma t}{\gamma} a(0) \right], \quad (\text{A1})$$

where  $C$  and  $\gamma$  are operators, given by

$$C = \frac{1}{2}\Delta\sigma_3 + \lambda(a^\dagger\sigma + \sigma^\dagger a) \quad (\text{A2})$$

and

$$\langle m, b | e^{iC(t_2-t_1)} | n, b \rangle = \delta_{n,m} \left[ \cos\mu'_n(t_1-t_2) + \frac{i\Delta}{2} \frac{\sin\mu'_n(t_1-t_2)}{\mu'_n} \right]. \quad (\text{A7})$$

Consider now a general initial state of the system,  $|\xi, \psi\rangle$ :

$$|\xi, \psi\rangle = \sum_n \langle n | \xi \rangle (\alpha | n, a \rangle + \beta | n, b \rangle), \quad (\text{A8})$$

where  $|\alpha|^2 + |\beta|^2 = 1$ . Using the results (A6) and (A7) we obtain, for the dipole-dipole correlation function (3),

$$\begin{aligned} \langle \xi, \psi | \sigma^\dagger(t_1)\sigma(t_2) | \xi, \psi \rangle &= \sum_{n=0}^{\infty} [ |\langle n | \xi \rangle|^2 |\alpha|^2 \langle n, a | \sigma^\dagger(t_1)\sigma(t_2) | n, a \rangle \\ &\quad + |\langle n+1 | \xi \rangle|^2 |\beta|^2 \langle n+1, b | \sigma^\dagger(t_1)\sigma(t_2) | n+1, b \rangle \\ &\quad + \alpha\beta^* \langle n | \xi \rangle \langle \xi | n+1 \rangle \langle n+1, b | \sigma^\dagger(t_1)\sigma(t_2) | n, a \rangle \\ &\quad + \alpha^*\beta \langle \xi | n \rangle \langle n+1 | \xi \rangle \langle n, a | \sigma^\dagger(t_1)\sigma(t_2) | n+1, b \rangle ]. \end{aligned} \quad (\text{A9})$$

Some of the summation indices have been renamed to make the state  $|n+1, b\rangle$  appear in all the matrix elements. This could be done because all the matrix elements involving the state  $|0, b\rangle$  are zero [see Eq. (A6b)]. Equations (A6) and (A7) may now be further used to cast Eq. (A9) into the form

$$\gamma = (C^2 + \lambda^2)^{1/2}. \quad (\text{A3})$$

It is clear that  $\gamma$  and  $C$  commute with each other. It is also clear that  $C$  is not diagonal in the basis of the atomic states and photon number states, but  $C^2$  [and, hence, by Eq. (A3),  $\gamma$ ] is. We have, from Eq. (A2),

$$C^2 = \frac{1}{4}\Delta^2 + \lambda^2(a^\dagger a + |a\rangle\langle a|). \quad (\text{A4})$$

The operator  $e^{iCt}$  which appears in Eq. (A1) may be written as

$$e^{iCt} = \cos Ct + i \frac{\sin Ct}{C} C, \quad (\text{A5})$$

where both  $\cos Ct$  and  $\sin Ct/C$  are even functions of  $C$  and therefore diagonal in the basis of atomic eigenstates and photon number states.

One can establish the following two basic results:

$$\begin{aligned} \sigma(t) | n, a \rangle &= e^{-i\omega_c t} \left[ \cos\mu_n t - \frac{i\Delta}{2} \frac{\sin\mu_n t}{\mu_n} \right] \\ &\quad \times e^{iCt} | n, b \rangle, \end{aligned} \quad (\text{A6a})$$

$$\sigma(t) | n, b \rangle = -ie^{-i\omega_c t} \lambda \sqrt{n} \frac{\sin\mu'_n t}{\mu'_n} e^{iCt} | n-1, b \rangle. \quad (\text{A6b})$$

Here  $|n, a\rangle$  ( $|n, b\rangle$ ) denotes a state with  $n$  photons and the atom in the upper (lower) state, and  $\mu_n$  and  $\mu'_n$  are the functions of  $n$  defined by Eqs. (7). Equations (A6) show how the calculations of average values such as (3) are reduced in any case to the calculation of the average value of  $e^{iC(t_2-t_1)}$  in the lower atomic state, which using (A5) and (A2) can be seen to reduce to

$$\begin{aligned}
\langle \xi, \psi | \sigma^\dagger(t_1) \sigma(t_2) | \xi, \psi \rangle &= \sum_{n=0}^{\infty} e^{i\omega_c(t_1-t_2)} \left[ \cos \mu'_n(t_1-t_2) + \frac{i\Delta}{2} \frac{\sin \mu'_n(t_1-t_2)}{\mu'_n} \right] \\
&\times \left[ \left[ \cos \mu_n t_1 + \frac{i\Delta}{2} \frac{\sin \mu_n t_1}{\mu_n} \right] \langle \xi | n \rangle_{\alpha^*} + i\lambda \sqrt{n+1} \frac{\sin \mu_n t_1}{\mu_n} \langle \xi | n+1 \rangle \beta^* \right] \\
&\times \left[ \left[ \cos \mu_n t_2 - \frac{i\Delta}{2} \frac{\sin \mu_n t_2}{\mu_n} \right] \langle n | \xi \rangle \alpha - i\lambda \sqrt{n+1} \frac{\sin \mu_n t_2}{\mu_n} \langle n+1 | \xi \rangle \beta \right]. \quad (\text{A10})
\end{aligned}$$

Now the first factor on the right-hand side of Eq. (A10) may be written as the sum of two terms which differ only by the sign of  $\mu'_n$ :

$$\cos \mu'_n(t_1-t_2) + \frac{i\Delta}{2} \frac{\sin \mu'_n(t_1-t_2)}{\mu'_n} = \frac{1}{2} \left[ 1 + \frac{\Delta}{2\mu'_n} \right] e^{i\mu'_n t_1} e^{-i\mu'_n t_2} + \frac{1}{2} \left[ 1 - \frac{\Delta}{2\mu'_n} \right] e^{-i\mu'_n t_1} e^{+i\mu'_n t_2}. \quad (\text{A11})$$

With this, Eq. (A10) may be written as the sum of two terms, each one of which is the product of a term containing  $t_1$  times its complex conjugate with  $t_2$  in place of  $t_1$ . Specifically, introducing the functions  $f_+$  and  $f_-$  defined as

$$f_+(\mu_n, \mu'_n, t) = \left[ 1 + \frac{\Delta}{2\mu'_n} \right]^{1/2} \left[ 1 + \frac{\Delta}{2\mu_n} \right] e^{i(\mu_n + \mu'_n + \omega_c)t}, \quad (\text{A12a})$$

$$f_-(\mu_n, \mu'_n, t) = \left[ 1 + \frac{\Delta}{2\mu'_n} \right]^{1/2} \frac{\lambda \sqrt{n+1}}{\mu_n} e^{i(\mu_n + \mu'_n + \omega_c)t}, \quad (\text{A12b})$$

Eq. (A10) may be written in the form

$$\begin{aligned}
&\langle \xi, \psi | \sigma^\dagger(t_1) \sigma(t_2) | \xi, \psi \rangle \\
&= \frac{1}{8} \sum_{n=0}^{\infty} \{ \alpha^* \langle \xi | n \rangle [f_+(\mu_n, \mu'_n, t_1) + f_+(-\mu_n, \mu'_n, t_1)] + \beta^* \langle \xi | n+1 \rangle [f_-(-\mu_n, \mu'_n, t_1) + f_-(-\mu_n, \mu'_n, t_1)] \} \\
&\quad \times \{ \alpha \langle n | \xi \rangle [f_+^*(\mu_n, \mu'_n, t_2) + f_+^*(-\mu_n, \mu'_n, t_2)] + \beta \langle n+1 | \xi \rangle [f_-^*(\mu_n, \mu'_n, t_2) + f_-^*(-\mu_n, \mu'_n, t_2)] \} \\
&\quad + (\text{same with } \mu'_n \rightarrow -\mu'_n). \quad (\text{A13})
\end{aligned}$$

To calculate the spectrum, Eq. (A13) must be substituted in Eq. (3) of the paper. After the integration over  $t_1$  and  $t_2$ , one obtains the sum of two products of complex conjugate terms, i.e., the sum of two absolute-value-squared terms (differing only by the sign of  $\mu'_n$ ) shown in Eq. (8). The functions  $F_n^{(+)}$  and  $F_n^{(-)}$  used there are readily seen to be due to the integrals of  $f_+$  and  $f_-$ , respectively.

\*Permanent address: Department of Physics, Miami University, Oxford, OH 45056.

†Permanent address: Department of Physics, Quaid-i-Azam University, Islamabad, Pakistan.

<sup>1</sup>For a survey of the current experimental and theoretical situation, see the special issues of *J. Mod. Opt.* **34**, Nos. 6/7 (1987); and *J. Opt. Soc. Am. B* **4**, No. 10 (1987).

<sup>2</sup>C. W. Gardiner, *Phys. Rev. Lett.* **56**, 1917 (1986).

<sup>3</sup>H. J. Carmichael, A. S. Lane, and D. F. Walls, *Phys. Rev. Lett.* **58**, 2539 (1987).

<sup>4</sup>H. Ritsch and P. Zoller, *Opt. Commun.* **64**, 523 (1987).

<sup>5</sup>J. Gea-Banacloche, *Phys. Rev. Lett.* **59**, 543 (1987).

<sup>6</sup>E. T. Jaynes and F. W. Cummings, *Proc. IEEE* **51**, 89 (1963).

<sup>7</sup>G. J. Milburn, *Opt. Acta* **31**, 671 (1984).

<sup>8</sup>P. Meystre and M. S. Zubairy, *Phys. Lett.* **89A**, 390 (1982). See also A. S. Shumovsky, F. L. Kien, and E. I. Aliskenderov, *ibid.* **124A**, 351 (1987).

<sup>9</sup>M. G. Raizen, L. A. Orozco, Min Xiao, T. L. Boyd, and H. J. Kimble, *Phys. Rev. Lett.* **59**, 198 (1987).

<sup>10</sup>K. Wódkiewicz, P. L. Knight, S. J. Buckle, and S. M. Barnett, *Phys. Rev. A* **35**, 2567 (1987).

<sup>11</sup>H. J. Carmichael, *Phys. Rev. Lett.* **55**, 2790 (1985).

<sup>12</sup>N. B. Narozhny, J. J. Sanchez-Mondragon, and J. H. Eberly, *Phys. Rev. A* **23**, 236 (1981).

<sup>13</sup>J. J. Sanchez-Mondragon, N. B. Narozhny, and J. H. Eberly, *Phys. Rev. Lett.* **51**, 550 (1983).

<sup>14</sup>G. S. Agarwal and R. R. Puri, *Phys. Rev. A* **33**, 1757 (1986); S. M. Barnett and P. L. Knight, *ibid.* **33**, 2444 (1986); G. S. Agarwal, R. K. Bullough, and G. P. Hildred, *Opt. Commun.* **59**, 23 (1986).

<sup>15</sup>J. R. Ackerhalt, Ph.D. thesis, University of Rochester, 1974; J. R. Ackerhalt and K. Rzażewski, *Phys. Rev. A* **12**, 2549 (1975).

<sup>16</sup>J. H. Eberly and K. Wódkiewicz, *J. Opt. Soc. Am.* **67**, 1252 (1977).

<sup>17</sup>B. R. Mollow, *Phys. Rev.* **188**, 1969 (1969).

<sup>18</sup>C. V. Sukumar and B. Buck, *Phys. Lett.* **83A**, 211 (1981); S. Singh, *Phys. Rev. A* **25**, 3206 (1982).

<sup>19</sup>P. Alsing and M. S. Zubairy, *J. Opt. Soc. Am.* **4**, 177 (1987).

<sup>20</sup>H.-I. Yoo and J. H. Eberly, *Phys. Rep.* **118**, 239 (1985); M. Brune, J. M. Raimond, and S. Haroche, *Phys. Rev. A* **35**, 154 (1987).

<sup>21</sup>J. Janszky and Y. Yushin, *Phys. Rev. A* **36**, 1288 (1987).